Water Soluble Nonionic Rosin Surfactants As Corrosion Inhibitor of Carbon Steel in 1 M HCl

G. A. El-Mahdy[*]*, Ayman M Atta and Hamad A. Al-Lohedan*

Chemistry department, College of Science, King Saud University, P.O.Box - 2455, Riyadh - 11451, Saudi Arabia.
[*]E-mail: gamalmah2000@yahoo.com

Preparation of nonionic surfactants from cheap biomaterials such as rosin and application in the field of corrosion inhibitors are the main goal of the present work. In this respect, rosin acids reacted with poly (ethylene glycol) monomethyl ether has molecular weight 750 g/mol, MPEG 750, to produce rosin ester (RMPEG-750). On the other hand, modification of rosin acid with maleic anhydride using Diles Alder reaction produced adduct (RMA) which esterified with MPEG 750 to produce branched nonionic surfactants to study the effect of rosin modification on both surface activity and corrosion inhibition efficiency in 1 M HCl. The surface activity of the prepared surfactants evaluated in deionized water and 1 M HCl to measure the micellization and adsorption of the prepared surfactants at water/air interface. The surface tension, critical micelle concentration, and surface activities were determined. Surface parameters such as surface excess concentration (Γ_{max}), the area per molecule at interface (A_{min}), and the effectiveness of surface tension reduction were determined from the adsorption isotherms of the prepared surfactants. The results of polarization measurements indicated that RMPEG750 acts as a mixed type inhibitor in acidic solution. The inhibition efficiency (IE) is dependent upon inhibitor concentration and increases with increasing inhibitor concentration. The charge transfer resistance of carbon steel increases with increasing inhibitor concentration and the corrosion process on CS surface is mainly controlled by charge transfer reaction.

1. INTRODUCTION

The development of renewable polymers is driven by carbon footprint reductions and a strong desire to shift away from our dependence on fossil fuels as organic material feedstocks [1-3]. The small share (<5%) of renewable polymers in the commercial market is largely due to high cost and inferior performance compared with synthetic polymers produced from petroleum chemicals. Some of

these polymers can be obtained entirely from nature. Rosin is a renewable natural resin obtained from the exudation of pine and conifer trees [4,5]. Rosin is one of the cheaper bio-based materials which can be used to replace the petrochemical products. It can be used to replace aromatic toxic compounds which used in the synthesis of polymeric surfactants. Although biobased polymeric surfactants based on rosin still have an insignificant share in the current marketplace dominated by fossil carbon based polymers, they are poised to grow rapidly in the near future. So far the development of rosin biobased polymers is mainly seen in the surfactant sector. On the other hand, the penetration of renewable feedstock into the synthesis of polymers has been relatively slow. Rosin consists primarily of abietic- and pimaric-type resin acids (or rosin acids) with characteristic hydrophobic hydrophenanthrene rings. Rosin acids have at least three unique important characteristics that most other natural biomasses lack: (1) they are a class of hydrocarbon-rich biomass, which can render hydrophobicity to any polymers attached; (2) they have a very bulky hydrophenanthrene group, which can significantly alter thermal properties of polymers integrated; and (3) rosin-derived esters are biocompatible because they are permitted to be used as food additives. Functionalization of the carboxyl group of rosin acids allows us to integrate rosin moiety into polymers as backbone or side chains [6-10].

Application of rosin in polymeric surfactants in the field of corrosion inhibitors and polymeric surfactants is rarely seen in the literature. It was previously [11] reported the preparation of dehydroabietates with poly(ethylene oxide). In an earlier study, nonionic polymeric surfactants based on rosin feedstock were prepared thought the esterification of rosin carboxylic groups of rosin with polyethylene glycol (PEG) having different molecular weights. Diels alder adducts of the produced rosin ester (reacted as diene) produced using maleic anhydride as dienophiles. The adduct reacted with diaminobutane or triethylene tetramine to produce rosin-imide [12]. Water-soluble surfactants based on rosin were prepared from condensed products of rosin –formaldehyde derivatives [13-15]. The derivatives were etherified with different molecular weights of PEG to prepare nonionic polymeric surfactants. The corrosion and corrosion inhibition of carbon steels in CO_2-saturated simulated formation water by rosin amide imidazoline (RAIM) was studied using electrochemical impedance spectroscopy and potentiodynamic polarization techniques [16]. In previous works [17] new corrosion inhibitors based on rosin poly(oxyethylene) ester 4,5-dihydroimidazole maleate adduct have been synthesized and evaluated s corrosion inhibitor for carbon steel in 1M hydrochloric acid solution was investigated using electrochemical methods. Data indicated that RIMA-PEG has shown a strong inhibitive effect for the corrosion of carbon steel in 1M HCl solution. Theoretical quantum chemical calculations data illustrated the mechanism for adsorption of RIMA-PEG molecules on carbon steel surface [18]. This work aims to increase the functionality of rosin acids such as the addition of reactive of carboxylic, anhydride groups to rosin. Our *approach* is to modify the chemical structure of rosin through reaction on both double bonds of fused ring structure and the carboxylic group of rosin to prepare new polymeric surfactants. We expect that the prepared rosin polymeric surfactants have not only possessed the high performance but also display high multipurpose additives as corrosion inhibitors. The present work is principally concerned with the addition reactions such as Diels Alder and alkoxylation reactions of this adducts and incorporation of the poly(ethylene glycol) derivatives into their structures. Therefore, modification of rosin acids which have carboxyl group and carbon-

carbon double bond can produce polymeric surfactants which may serve as alternative materials to the perochemical-based- surfactants.

2. EXPERIMENTAL

Rosin acids with acid number 183mg KOH.g^{-1} and melting point 167°C was obtained from commercial rosin. Rosin were heated at 150°C for 4 hours then heated at 200°C for 30 minutes in nitrogen atmosphere to isomerizes rosin acids to leveopimaric acid, then it were separated by crystallization from the cold acetone solution of commercial rosin. The separation of the rosin acids from rosin was carried out to increase the yield and to remove terpens, which have the ability to react with maleic anhydride. Maleic anhydride (MA), p-toluene sulfonic acid (PTSA), poly (ethylene glycol) monomethyl ether, PEGME, has molecular weight 750 were supplied from Aldrich Chemicals Co. (USA) and used as received. The corrosive solution (1M HCl) was prepared by appropriate dilution of analytical grade 37% HCl with double distilled water.

2.1. Esterification of rosin

A four-necked flask fitted with a condenser was charged with 1 mol of rosin acid, 1mol of MPEG750 and 1% PTSA by weight as a catalyst. The esterification reaction was carried out under a slow stream of deoxygenated nitrogen, the reaction was agitated using mechanical stirrer at 500 rpm. Then a Dean- Stark seperator was fitted to the flask and the reaction mixture was carried out by heating at 200°C untill all water of esterification is removed. Unreacted MPEG 750 was removed by dissolving the prepared surfactant in isopropanol with ratio 1 :1 followed by adding hot concentreted solution of NaCl at 60-70 °C in separating funnel. The prepared surfactant was dried in the oven at 70°C for 1hour.

Rosin MEG ester- maleic anhydride adducts with MPEG750 can be designated as RMPEG 750

2.2. Esterification of RMA-MPEG 750

Rosin 100 g was added into a three necks round bottom flash equipped with mechanical stirrer, thermometer, condenser and nitrogen inlet. The gum rosin was heat to 180 ^{o}C and maintained at this temperature for 1 h under the nitrogen atmosphere. 30 g maleic anhydride was then added and stirred at 180 ^{o}C for 3 h followed by raising the temperature to 220 ^{o}C and maintaining for 1 h. The reaction was cooled to 100 oC and 200 ml acetic acid was added. After the temperature was cooled to room temperature, the yellow solid Rosin-MA adduct (RMA) was obtained. The crude product was recrystallized twice from acetic acid and obtained 55 g white crystal. RMA (1 mol) was heated with 3.1 mol of MPEG 750 and 1% PTSA by weight as a catalyst in the presence of nitrogen gas. The Dean- Stark separator was fitted to the flask and the reaction mixture was carried out by heating at 120°C until all water of esterification is removed. Unreacted MPEG 750 was removed by salting out

through dissolving the prepared surfactant in isopropanol with ratio 1 :1 followed by adding hot concentrated solution of NaCl at 60-70 °C in separating funnel. The prepared surfactant was dried in the oven at 70°C for 1hour.

RMA ester with MPEG750 can be designated as RMA-(MPEG 750)$_3$

2.3. Characterization of the prepared Surfactants:

FTIR spectra were analyzed with a Nicolet FTIR spectrophotometer using KBr in a wavenumber range of 4000–500 cm^{-1} with a resolution accuracy of 4 cm^{-1}. All samples were ground and mixed with KBr and then pressed to form pellets.

The surface and interfacial tension measurements between water solution and styrene was measured at 25 ^{o}C by means of the pendent drop technique using drop shape analyzer model DSA-100 (Kruss, Germany). In this method the shape of a pendent drop is fitted to the theoretical drop profile according to the Laplace equation, using surface tension as one of the adjustable parameters. The error limits of these measurements are on the order of 0.1 mN/m or less. The ADSA-100 analysis required accurate density measurements, which were measured as functions of temperature and nanogels concentration with an AP Paar DMA45 MC 1296 densitometer. Pendent drops were formed on the tip of a Teflon capillary with an outside diameter of 0.1 in. and inside diameter of 0.076 in.

2.4. Electrochemical measurement

A standard three-electrode electrochemical/corrosion cell was utilized in all electrochemical experiments. The counter electrode was a platinium electrode. The reference electrode was a Ag/AgCl. The working electrode was prepared from a carbon steel (CS) sealed with an exposed area (0.1 cm^2) to the electrolyte. Electrochemical measurements and EIS impedance measurements were performed using a Solartron 1470E system (potentiostat/galvanostat) with Solartron 1455A as frequency response analyzer. Multistate software was used to run the tests, collect and evaluate the experimental data. Impedance tests were performed in 1M HCl with and without inhibitor. The impedance data were analyzed and fitted with the simulation ZView 3.3c , equivalent circuit software.

3. RESULTS AND DISCUSSION

The physical properties of rosin acids including melting temperature and acid number are 161°C and 183 mg KOH/ g of resin acid, respectively. These values indicate that the separated rosin acids are in form of abietic and levopimaric acid. The present work deals with synthesis of nonionic surfactants by reacting the carboxylic acid of rosin acid with MPEG-750. The strategy of synthesis is based on preparation of nonionic surfactants having different hydrophile-lipophile balance (HLB) to study effect of surfactant structure on its properties.

The rosin acids was esterified with MPEG 750 to increase hydrophilicity of rosin acids. On the other hand, RMA was reacted with MPEG 750 to study the effect of increasing MPEG 750 content on the hydrophilicity of the prepared surfactants. The structures of the produced surfactants were confirmed by using FTIR spectroscopy. Accordingly, a representative infrared spectral patterns of RMA and RMPEG 750 were represented in Figure 1.
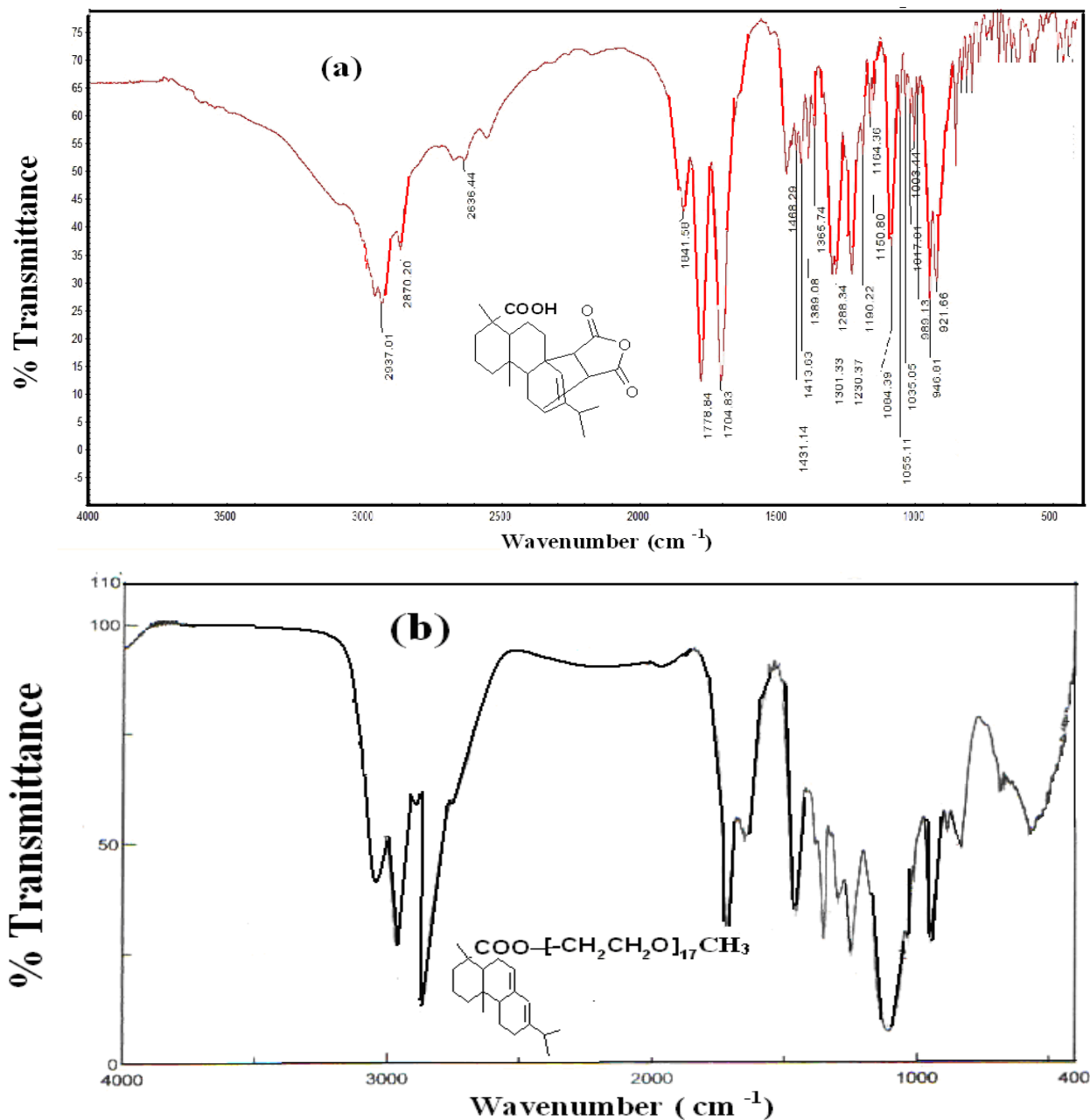

Figure 1. FTIR Spectra of a) RMA and b) RMA-(MPEG 750)$_3$

It was observed that the spectrum of RMA-(MPEG 750)$_3$ is nearly identical. The disapperance of two stretching bands at 1810 and 1780 cm^{-1}, represented C=O anhydride group) and apperance of

stretching bands at 1745 cm^{-1} for carbonyl (C=O) of ester and the band at 1110 cm^{-1} for C-O ester are observed in spectra of RMA-(MPEG 750)$_3$ and RMPEG 750.

3.1 Surface Activity of the prepared surfactants

Although knowledge of surface and interfacial properties is important for application of surfactants as corrosion inhibitors but almost paper measure the surface properties in distilled water and evaluate the corrosion inhibition efficiencies either in acidic or salt water [19, 20]. The correlation between surface tension measured in distilled water with the corrosion inhibition is not accurate to apply. In this respect the surface tension will be evaluated in both distilled water in 1 M HCl to study the adsorption characteristics at air/water interface and micellization of the surfactants in bulk solutions either in distilled or acidic aqueous solutions. In the present work, the dynamic surface tension of the two prepared surfactants RMPEG750 and RMA-(MPEG 750)$_3$ were measured at water/air interface by variation their concentrations at temperature of 25 $^{\circ}$C. The relation between the surface tension of R-MPEG 750 in 1 M HCl aqueous solutions and time at different concentrations were represented in figure 2 as representative samples.
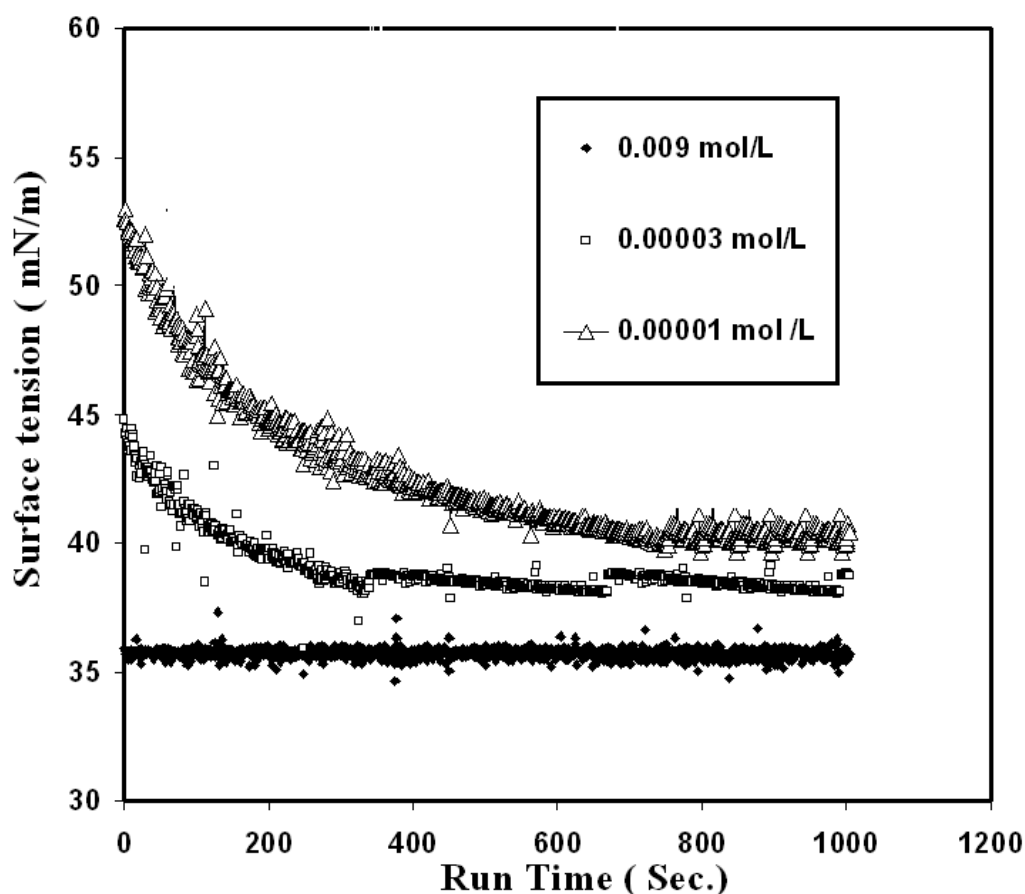

Figure 2. Relation between surface tension of R-MPEG 750 and time different concentrations in 1M aqueous HCl solutions.

The data illustrated in figure 2 indicated the surfactants reached the equilibrium after different time intervals (ranged from 10 to 15 minutes) when the concentration lowered than 6 x 10 $^{-5}$ mol/L (800 ppm). These data proved that the prepared surfactants highly adsorbed at air/water interface. It is well known that he micellization, aggregation and adsorption of surfactants are based on the critical micelle concentrations (cmc), which were determined by the surface balance method as represented in figure 3.
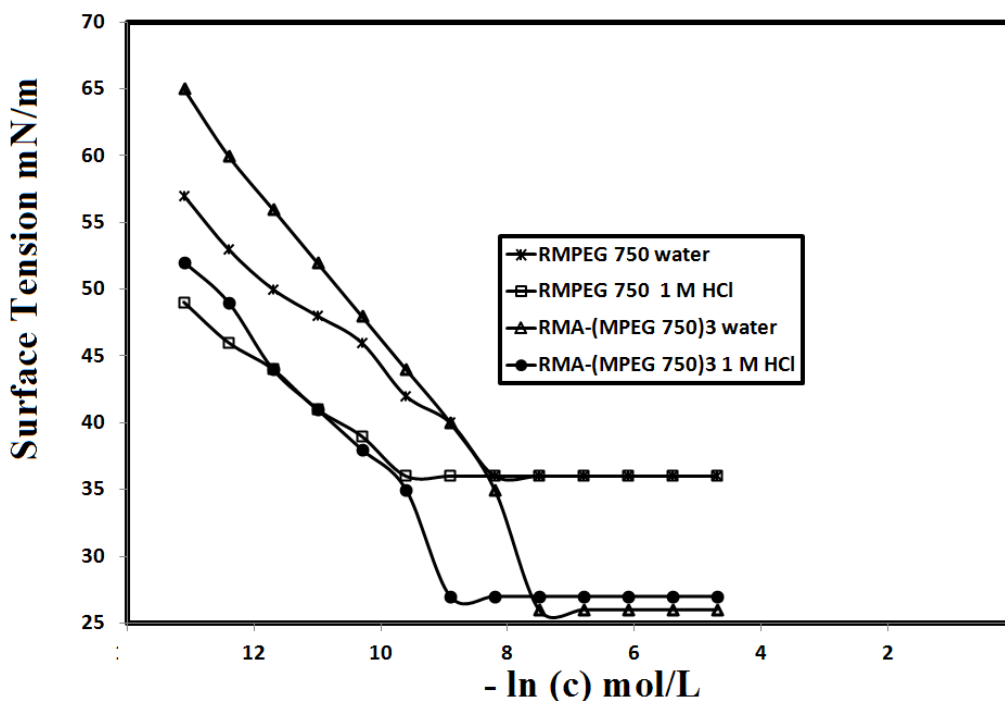

Figure 3. Adsorption isotherms of RMPEG 750 and RMA-(MPEG 750)$_3$ in distilled water and 1 M HCl solutions at 25 ^{o}C.

Table 1. Surface properties of the RMPEG750 and RMA- (MPEG)$_3$ in distilled water and 1 M HCl solutions at 25 ^{o}C.

Designation	cmc mol/L x 10^4		γ_{cac} mN/m		$(-\partial \gamma / \partial \ln c)$		Γ_{max} x 10^{10} mol/ cm^2		A_{min} nm^2/molecule	
	water	1M HCl	water	1M HCl	water	1M HCl	water	1M HCl	water	1M HCl
RMPEG750	1.5	0.41	36.2	36.2	3.6	3.2	1.4	1.29	0.232	0.214
RMA-(MPEG)$_3$	2.4	0.62	25.6	26.1	5.9	5.2	2.4	2.10	0..398	0.349

The cmc values of the prepared surfactants were determined in water and 1 M HCl aqueous solution at 25 ^{o}C from the change in the slope of the plotted data of surface tension (γ) *versus* the

solute concentration (ln C) and listed in table 1. The data indicated that the cmc values were reduced when 1 M HCl used instead of water, which indicated that the solubility of the surfactants altered with HCl and indicated that the adsorption micellization of the prepared surfactants occurred at lower concentration in 1 M HCl. The intersection in the surface tension curves can be used to determine cmc values of the prepared surfactants and the corresponding surface tension is defined as γ_{cmc}. The effectiveness of the prepared surfactants was expressed by the maximum reduction of surface tension of the organic solvents which calculated from the equation, $\Delta\gamma = \gamma_{water} - \gamma_{cmc}$. The $\Delta\gamma$ values of the prepared surfactants were determined and listed in Table 1. The differences in surface activity of surfactants are based on the high adsorption of prepared surfactants at the air/water interface. A possible explanation seems reasonable to propose that surface tension data involves two processes the adsorption of prepared surfactants to the interface and the unfolding of surface tails and loops to cover the entire interface. The amount of the prepared surfactants adsorbed per unit area of liquid–gas or liquid–liquid interface, although possible, is not generally undertaken because of the difficulty of isolating the interfacial region from the bulk phase for purposes of analysis when the interfacial region is small, and of measuring the interfacial area when it is large. The orientation and packing of the prepared surfactants molecules at the air/water interface prominently depend upon the molecular structure, and extent of association of the prepared surfactants and solvent molecules as described in the previous section. In this respect, the amount of the prepared surfactants adsorbed per unit area of interface is calculated indirectly from the surface or interfacial tension measurements. The concentration of the prepared surfactants at the solvent–air interface can be calculated as surface excess concentration Γ_{max}. The surface excess concentration of the prepared surfactants at the interface can be calculated from surface or interfacial tension data using the following equation: $\Gamma_{max} = 1/RT \times (-\partial\gamma / \partial \ln c)_T$, where $(-\partial\gamma / \partial \ln c)_T$ is the slope of the plot of γ *versus* ln c at constant temperature (T) and R is the gas constant (in J mol^{-1} K^{-1}). The surface excess concentration at surface saturation is a useful measure of the effectiveness of adsorption of the prepared surfactants at the liquid–gas or liquid–liquid interface, since it is the maximum value that adsorption can attain. The Γ_{max} values were used for calculating the minimum area A_{min} at the aqueous–air interface. The area per molecule at the interface provides information on the degree of packing and the orientation of the adsorbed surfactants, when compared with the dimensions of the molecule as obtained from models. From the surface excess concentration, the area per molecule at the interface is calculated using the equation: $A_{min} = 10^{16}/ N \Gamma_{max}$, where N is Avogadro's number. The data of Γ_{max}, A_{min}, and $(-\partial\gamma / \partial \ln c)$ were determined and listed in Table 1. As shown in Table 1, A larger Γ_{max} means that more molecules adsorbed on the surface of the solution, which also means a lower surface tension. However, a low A_{min} data suggest compact adsorption of of the prepared surfactants at interface or complete surface coverage by the prepared surfactants. The obtained results were listed in Table 1. The reduction of surface tension, and A_{min} of the prepared surfactants in 1 M HCl indicate that the prepared compound gives large reduction of surface tension at cmc, so that, the compound acts as effective corrosion inhibitor for mild steel in 1M HCl solution.

3.2. Electrochemical impedance spectroscopy

The electrochemical impedance spectroscopy (EIS) is a powerful technique in studying corrosion mechanisms and adsorption phenomena Hence, EIS technique was employed to investigate the electrode/electrolyte interface and the electrochemical processes occur on the CS surface in the presence and absence of inhibitor in 1 M HCl solution.
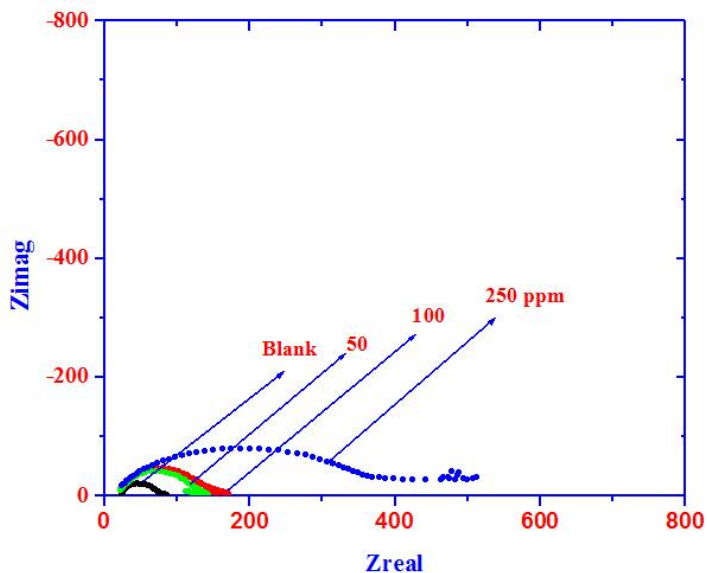

Figure 4. Nyquist plots for CS in 1 M HCl containing RMPEG750   with different concentrations.
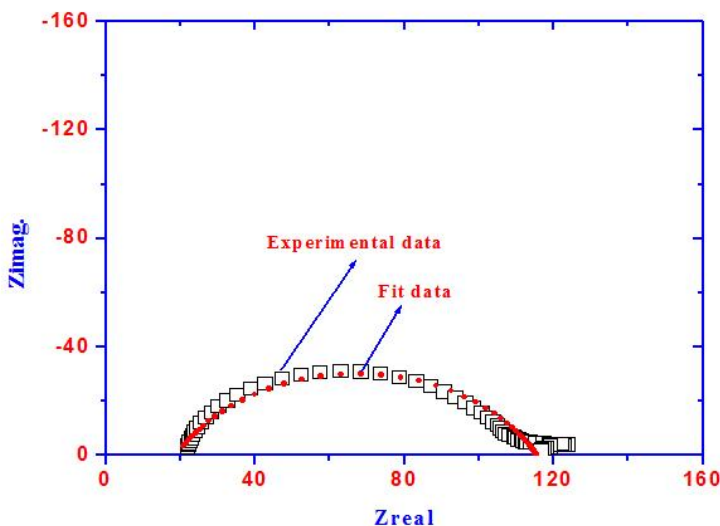

Figure 5. Nyquist plots for CS in 1 M HCl containing RMA- (MPEG)$_3$ showing experimental and fit data.

Fig. 4 shows the Nyquist plots for carbon steel in 1 M HCl solution in the absence and presence of RMPEG750 as   inhibitor at various concentrations. The measurements were made after the stabilization of the electrode at OCP for one hour. The figure shows that the diameter of the semicircle increases with the increasing   inhibitor concentration in the electrolyte and the Nyquist plots were not

perfect semicircles. Figure 5 shows the Nyquist plot for carbon steel in 1M HCL solution containing 250 ppm of RMA- (MPEG)$_3$ as derivative of RMPEG750 .
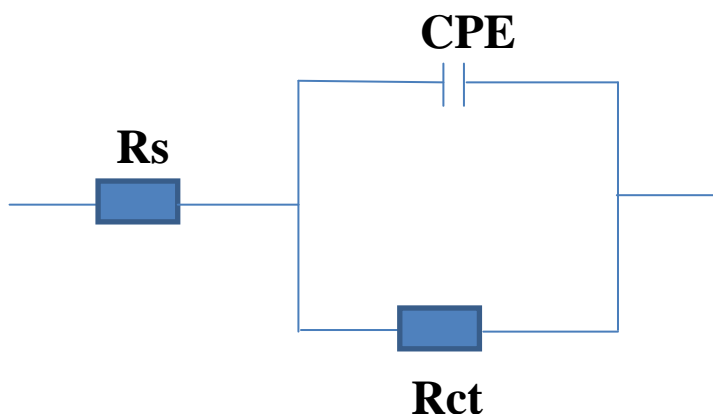

Figure 6. Equivalent circuit used for fitting impedance spectra

The EIS data were analyzed by fitting to the equivalent circuit model shown in Fig.6, which fits the experimental results. The circuits comprise a solution resistance Rs, in series with the constant phase element CPE, which in turn in parallel with charge transfer resistance (Rct). The data indicated that the corrosion of CS in 1 M HCl solution mainly controlled by a charge-transfer process [21–25]. The CPE can be modeled as follows [26-28]. The CPE is defined by the mathematical expression [27-28]:

$$Z_{CPE} = 1 / Y_o (j\omega)^n \tag{1}$$

where Z_{CPE}, impedance of CPE; Y_o, a proportional factor; ω, Angular frequency ($\omega = 2\pi f$, where *f* is the AC frequency) and j is the imaginary unit (the square root of -1). Depending upon the values of n, CPE may be resistive to n = 0, capacitance for n = 1, Warburg's impedance for n = 0.5 or an inductance for n = -1. and n the exponential term, which has many different explanations, it can be associated with the roughness of electrode surface [29], a distribution of reaction rates [28], non-uniform current distribution [30-31]. Depending on n, CPE can represent resistance ($Y_o = R$, n = 0), capacitance ($Y_o = C$, n = 1), inductance ($Y_o = L$, n = -1) or Warburg impedance (n = 0.5, $Y_0 = W$). As it is shown in Table 1, the values of Rct increase with increasing inhibitor concentration, which suggests that more inhibitor molecules are adsorbed on the CS surface at higher concentration leading to greater surface coverage. The adsorption of the inhibitor on the CS surface decreases its electrical capacity because they displace the water molecules and other ions originally adsorbed on the surface [32–34]. This fact suggests that the inhibitor molecules act by adsorption at the CS surface /solution interface [35]. The inhibition efficiency (EI) was calculated using the charge transfer resistance as follow [35]:

$$\% IE = (1 - R_{ct} / R^*_{ct}) \times 100 \tag{2}$$

where R^*_{ct} and R_{ct} are the charge-transfer resistances with and without inhibitors, respectively. %IE was calculated and listed in Table 2. It can be concluded from the EIS data that a high protection was observed at high inhibitor concentration, which can be accounted to more adsorption of the inhibitor on the CS surface.

Table 2. Dependence of inhibitor efficiency (IE) on RMPEG750 concentration calculated by EIS technique.

Concentration (ppm)	Rct (ohm cm^2)	%IE
Blank	59	__
50 (RMPEG750)	120	50.83
100 (RMPEG750)	218	72.93
250 (RMPEG750)	489	87.93
250 (RMA- (MPEG)$_3$)	96.56	38.8

3.3.Polariztion measurements

Polarization measurements were conducted to determine the inhibitr efficiency and verify the data obtained from EIS measurements.
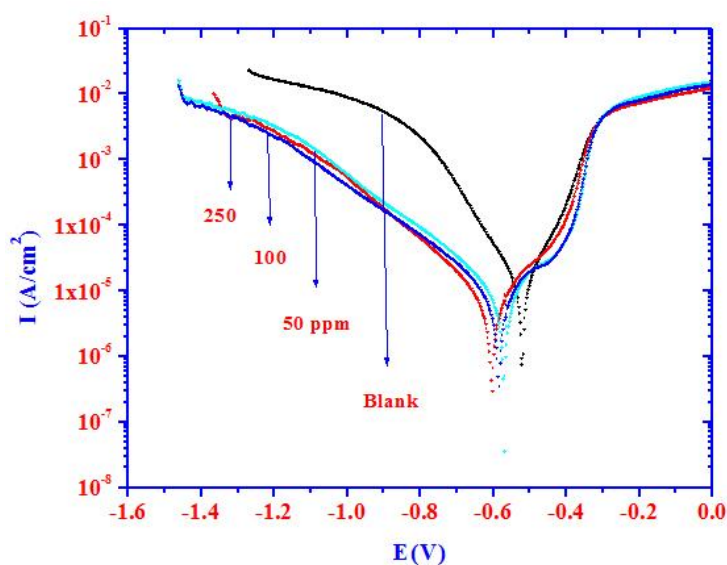

Figure 7. Polarization curves for carbon steel measured in 1M HCl solution containing RMPEG750 with different concentrations.

Figure 7 shows polarization curves recorded on a CS electrode 1 M HCl solution, in absence and presence of RMPEG750 as inhibitor at various concentrations. Figure 8 shows the polarization curve for carbon steel in 1M HCL solution containing 250 ppm of RMA- (MPEG)$_3$ as derivative of RMPEG750. The results indicate that inhibitor acts as mixed-type corrosion inhibitor. In acidic solutions, the anodic reaction of corrosion is the passage of metal ions from the metal surface into the

solution, and the cathodic reaction is the discharge of hydrogen ions to produce hydrogen gas or to reduce oxygen. The inhibitor may affect either the anodic or the cathodic reaction, or both [36]. The addition of inhibitor molecules has an inhibitive effect in the both anodic and cathodic parts of the polarization curves as evident from the data presented in Fig.
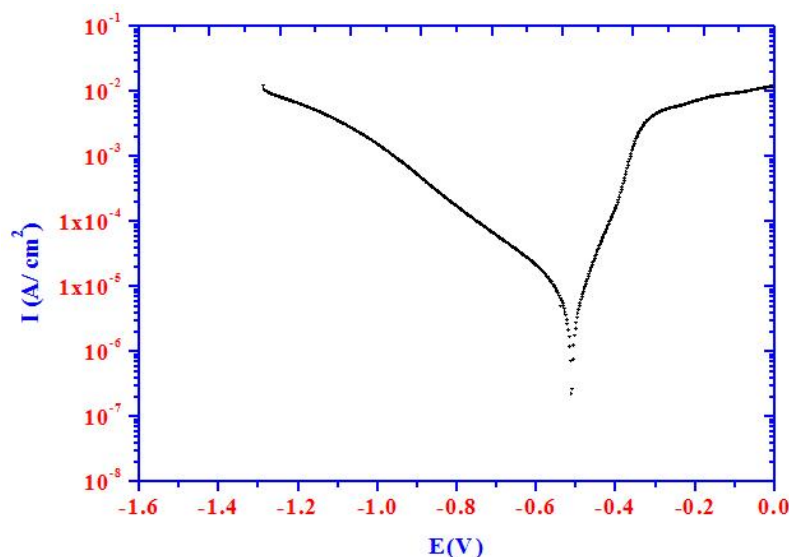

Figure 8. Polarization curves for carbon steel measured in 1M HCl solution containing RMA-(MPEG)$_3$.

It is clear that with an increase in inhibitor concentration in the bulk solution, both the cathodic and anodic current decreases. This may be ascribed to adsorption of the inhibitor over the metal surface. Therefore, inhibitor molecules can be arranged as a mixed-type inhibitor [37-38]. The suppression of the cathodic process can be attributed to the adsorption of inhibitor molecules on the cathodic sites [39]. The corrosion current decreased slightly during the initial stage of anodic polarization, which enhanced predominantly with a shift in potential to the positive potential. The results indicated that the adsorption rate was higher than the desorption rate of inhibitor molecules on CS surface. It can be concluded that the adsorption process dominated the anodic reaction. Thus, addition of this inhibitor reduces the CS dissolution as well as delaying the hydrogen evolution reaction.

The corresponding corrosion current is presented in Table 3 together with the corresponding inhibition efficiency, which was calculated using the following equation [40-45]:

$$\%IE = (1 \; - \; i^o_{corr} / i_{corr}) \; x \; 100 \tag{3}$$

where i_{corr} and i^o_{corr} are corrosion current densities in absence and presence of inhibitor, respectively, determined by extrapolation of cathodic current potential lines to corrosion potential. %IE was estimated for CS and quoted in Table 3.

Table 3. Dependence of inhibitor efficiency (IE) on inhibitor concentration calculated by electrochemical technique.

Concentration (ppm)	I (mA/cm^2)	% IE
Blank	0.168	__
50 (RMPEG750)	0.071	57.73
100 (RMPEG750)	0.045	73.2
250 (RMPEG750)	0.015	91.10
250 (RMA- (MPEG)$_3$)	0.092	45.23

It can be concluded that the anodic iron dissolution and cathodic hydrogen evolution reaction were both inhibited by the addition of inhibitor through merely blocking the reaction sites of CS surface. In addition, as the inhibitor concentration increased, the corrosion rate decreased due to more inhibitor adsorption of inhibitor on the CS surface. The lower value of % IE experienced by RMA-(MPEG)$_3$ that that produced by RMPEG750 may be attributed to the different in mode of adsorption. The inhibitor molecule of RMPEG750 was adsorbed in parallel mode to the CS surface, which cover most CS surface, while RMA- (MPEG)$_3$ molecule was adsorbed in perpendicular mode , which partly cover the CS surface and leads to lower value of IE.

4. CONCLUSIONS

The following conclusions can be withdrawn from the discussed results:

1- The data indicated that the prepared rosin surfactants (RMPEG-750 and RMA-(MPEG750)$_3$) reached the equilibrium after different time intervals (ranged from 10 to 15 minutes) when the concentration lowered than 6 x 10^{-5} mol/L (800 ppm).

2- The cmc values of the prepared surfactants were reduced when 1 M HCl used instead of water, which indicated that the solubility of the surfactants altered with HCl and indicated that the adsorption micellization of the prepared surfactants occurred at lower concentration in 1 M HCl.

3- RMPEG750 as nonionic rosin surfactants surfactant acts as a good inhibitor for the corrosion of CS in 1 M HCl and its inhibition efficiency is dependent upon inhibitor concentration and increases with increasing inhibitor concentration.

4- The results of potentiodynamic polarization indicate that RMPEG750 behave as mixed -type corrosion inhibitor.

5- The corrosion process on the CS surface can be monitored by EIS and is mainly controlled by charge transfer reaction.

References

1. W.Coates, M. A. Hillmyer, *Macromolecules* 42 (2009)7987.

2. M. Okada, *Prog. Polym. Sci.* 27 (2002) 87–133.
3. A. J. Ragauskas, C. K. Williams, B. H. Davison, G.Britovsek, J. Cairney, C. A. Eckert, W. J. Frederick, J. P. Hallett, D. J.Leak, C. L. Liotta, J. R. Mielenz, R. Murphy, R. Templer, T.Tschaplinski, *Science* 311(2006)484–489.
4. S. Maiti, S. S. Ray, A. K. Kundu, *Prog. Polym. Sci.* 14 (1989) 297.
5. R. S. Sinha A. K. Kundu, S. Maiti, *Eur. Polym. J.* 26 (1990) 471.
6. A. M. Atta, I. F. Nassar, H. M. Bedawy, *React. Funct. Polym.* 67 (2007)617.
7. Y. Zhang, R. J. Heath, D. J. Hourston, *J. Appl. Polym. Sci.* 75 (2000) 406.
8. J. S. Lee, S. I. Hong, *Eur. Polym. J.* 38 (2002) 387.
9. Y. Zheng, K.Yao, J. Lee, D. Chandler, J. Wang, C.Wang, F. Chu, C. Tang, *Macromolecules* 43 (2010) 5922.
10. P. A. Wilbon, Y. Zheng, K. Yao, C. Tang, *Macromolecules* 43(2010) 8747.
11. S. P. Piispanen, U. R. M. Kjellin, B. Hedman, T. Norin, *J. Surf. Deterg.* 6 (2003)125.
12. A. M. Atta, A. M. Ramadan, K. A. Shaffei, A. M. Nassar, M.Fekry, *J. Dispers Sci. Technol.* 30 (2009) 1100.
13, A. M. Atta, A. M. Elsaeed, *J. Appl. Polym. Sci.* 122 (2011)183.
14. A. M. Atta, A. F. El-Kafrawy, M.E. Abdel-Rauf, N. E. Maysour, A. K. Gafer, *J. Dispers Sci. Technol.* 31(2010) 567.
15. A. M. Atta, M.E. Abdel-Rauf, N. E. Maysour, A.K. Gafer, *J. Dispers Sci. Technol.*31 (2010) 583.
16. P. C. Okafor, C. B. Liu, Y. J. Zhu, Y. G. Zheng, *Ind. Eng. Chem. Res.* 50 (2011) 7273.
17. A. M. Atta, , G. A. El-Mahdy, H. S. Ismail, H. A. Al-Lohedan, *Int. J. Electrochem. Sci.*, 7 (2012) 11834.
18. A. M. Atta, G. A. El-Mahdy, A. A. Al-Azhary, H. A. Al-Lohedan, *Int. J. Electrochem. Sci.,* 8 (2013) 1295.
19. A.M. Badawia, M.A. Hegazya, A.A. El-Sawyb, H.M. Ahmeda, W.M. Kamela, *Mat. Chem. Phys*. 124 (2010) 458.
20. A.M. Alsabagh, M.A. Migahed, H. S. Awad, *Corros. Sci*. 48 (2006) 813.
21. M. El Achouri, S. Kertit, H.M. Gouttaya, B. Nciri, Y. Bensouda, L. Perez, M.R. *Prog. Org. Coat*. 43 (2001) 267.
22. M. Erbil, *Chim. Acta Turc*. 1 (1988) 59.
23. I. Dehri, H. Sozusaḡlam, M. Erbil, *Prog. Org. Coat*. 48 (2003) 118.
24. F. Bentiss, B. Mernari, M. Traisnel, H. Vezin, M. Lagrenee, *Corros. Sci*. 53 (2011) 487.
25. A. Chetouani, A. Aouniti, B. Hammouti, N. Benchat, T. Benhadda, S. Kertit, *Corros. Sci*. 45 (2003) 1675.
26. D.F. Roeper, D. Chidambaram, C.R. Clayton, G.P. Halada, *Electrochim. Acta* 53 (2008) 2130.
27. H. Ashassi-Sorkhabi, D. Seifzadeh, M.G. Hosseini, *Corros. Sci*. 50 (2008) 3363.
28. D.F. Roeper, D. Chidambaram, C.R. Clayton, G.P. Halada, *Electrochim. Acta* 53 (2008) 2130.
29. W.H. Mulder, J.H. Sluyters, T. Pajkossy, L. Nyikos, *J. Electroanal. Chem*. 285 (1990) 103.
30. C.H. Kim, S.I. Pyun, J.H. Kim, *Electrochim. Acta* 48 (2003) 3455–3463.
31. J.B. Jorcin, M.E. Orazem, N. Pebere, B. Tribollet, *Electrochim. Acta* 51 (2006) 1473.
32. M.A. Amin, K.F. Khaled, S.A. Fadl-Allah, *Corros. Sci*. 52 (2010) 140.
33. G. Avci, *Mater. Chem. Phys*. 112 (2008) 234.
34. K.F. Khaled, *Mater. Chem. Phys*. 112 (2008) 290.
35. H. Ashassi-Sorkhabi, B. Shaabani, D. Seifzadeh, *Electrochim. Acta* 50 (2005) 3446.
36. V. Ramesh Saliyan, A.V. Adhikari, *Corros. Sci.* 50 (2008) 55.
37. G.N. Mu, X.H. Li, Q. Qu, J. Zhou, *Corros. Sci*. 48 (2006) 445.
38. S. Issaadi, T. Douadi, A. Zouaoui, S. Chafaa, M.A. Khan, G. Bouet, *Corros. Sci.* 53 (2011) 1484.
39. K.F. Khaled, M.M. Al-Qahtani, *Mater. Chem. Phys*. 113 (2009) 150.
40. F. Bentiss, M. Lagrenee, M. Traisnel, *Corrosion* 56 (2000) 733.
41. S. Omanovic, S.G. Roscoe, *Corrosion* 56 (2000) 684.

42. V. Hluchan, B.L. Wheeler, N. Hackerman, *Werk, Korro.* 39 (1988) 512.
43. M.A. Amin, S.S. Abd El Rehim, H.T.M. Abdel-Fatah, *Corros Sci*. 51 (2009) 882.
44. M.A. Migahed, M. Abd-El-Raouf, A.M. Al-Sabagh, H.M. Abd-El-Bary, *Electrochim. Acta* 50 (2005) 4683.
45. F. Bentiss, M. Traisnel, N. Chaibi, B. Mernari, H. Vezin, M. Lagrenee, *Corros. Sci.* 44 (2002) 227.